Diamond & Related Materials 61 (2016) 1–6

Contents lists available at ScienceDirect

Diamond & Related Materials

journal homepage: www.elsevier.com/locate/diamond

Time-stability of a Single-crystal Diamond Detector for fast neutron beam diagnostic under alpha and neutron irradiation

M. Rebai [a,b,*], A. Fazzi [c], C. Cazzaniga [d], G. Croci [b], M. Tardocchi [b], E. Perelli Cippo [b], C.D. Frost [d], D. Zaccagnino [c], V. Varoli [c], G. Gorini [a,b]

[a] University of Milano Bicocca, Piazza della Scienza 3, 20126 Milano, Italy
[b] IFP-CNR, Via Cozzi 53, 20125 Milano, Italy
[c] Department of Energy of the Politecnico di Milano, via Lambruschini 4,20156 Milano, Italy
[d] STFC, Rutherford Appleton Laboratory, Didcot, OX11 0QX, United Kingdom

ARTICLE INFO

Article history:
Received 3 September 2015
Received in revised form 21 October 2015
Accepted 5 November 2015
Available online 10 November 2015

ABSTRACT

Single-crystal Diamond Detectors (SDDs), due to their good charge carrier transport properties, low leakage and therefore good energy resolution, are good candidates for fast neutron measurement on pulsed spallation sources and fusion plasma experiments. Moreover, diamonds are known to be resistant to neutron irradiation. Nevertheless, measurements show transient effects during irradiation with ionizing particles, as the alpha particle calibration sources. The decrease of the detector counting rate of a counting chain and the pulse height are interpreted as due to a charge trapping inside the detector, which modifies the drift electric field. These instabilities are strongly dependent on the specific type of the interaction. Measurements have been carried out with both alpha particles in the laboratory and neutrons at the ISIS neutron spallation source. We show that these polarization effects are not permanent: the detector performances can be restored by simply inverting the detector bias high voltage.

Prime Novelty Statement: The measurements described in the paper were performed in order to study the polarization effect in Single-crystal Diamond Detector. This effect was observed under alpha particle and neutron irradiation. With the Transient Current Technique an interpretation of the effect is given.

1. Introduction

Artificial single-crystal diamonds are applied as fast neutron detectors for application on spallation sources and fusion experiments.

A new beam line, named ChipIR [1] was built at the ISIS spallation neutron source (UK). This beam line is characterized by an atmospheric-like neutron spectrum with a fast ($E_n > 10$ MeV) neutron mean flux about 10^8–10^9 times more intense than the atmospheric one at ground level. This will allow single event effects study on electronic devices [2,3]. Single-crystal Diamond Detectors (SDDs), due to their high radiation hardness, fast response and small size, are good candidates as ChipIR beam monitors [4,5,6].

Diamond Detectors are of particular interest also for high resolution and high rate neutron spectroscopy for diagnostics of fusion plasmas, as it has been demonstrated by measurements at the JET tokamak [7–9]. A new detector based on a matrix of SDDs has been developed and it was installed at JET [10–13].

Neutron detection with SDDs is based on the collection of electron–hole pairs produced by the charged particles generated by the neutron interaction on ^{12}C. The main reactions occurring in carbon are:

- the n-α reaction: $^{12}C(n\text{-}\alpha)^9Be$, $Q_{value} = -5.7$ MeV, $E_{thr} = 6.17$ MeV;
- the elastic neutron scattering channel: $^{12}C(n,n')^{12}C$;
- the n-3α reaction (carbon breakup): $^{12}C(n,n')3\alpha$ ($Q_{value} = -7.23$ MeV, $E_{thr} = 7$ MeV.

The energy released into the detector is directly related to the neutron energy only in the first reaction, where the energy of the secondary products can be calculated and if the ionization range of these product is lower than the detector thickness, all their energy is released into the detector. The other two reactions, due to kinematics, give rise to a continuum of energies.

The pulses are then amplified and sent to a threshold discriminator followed by a pulse counter. A crucial point for the development of a beam monitor is the counting stability along time. Tests have been performed in order to study the detector stability during both neutron and charged particle irradiation. In this paper some recent stability experiments performed with SDD coupled to an alpha particle emitter

* Corresponding author at: University of Milano Bicocca, Piazza della Scienza 3, 20126 Milano, Italy.
E-mail address: marica.rebai@mib.infn.it (M. Rebai).

http://dx.doi.org/10.1016/j.diamond.2015.11.002
0925-9635/

will be described, and compared to neutron measurements. The main results can be summarized as follows:

a) In the case of alpha particles the counting rate substantially decreases after a period, here called polarization time; in Section 3a a description of the phenomenon is accounted for. The polarization time results to be dependent on the applied bias and the particle fluence.
b) In the case of neutrons this effect does not happen even for measurement times much longer than the alpha particles one (Section 3b).
c) The waveforms recorded with alpha particles show a significant and systematic changing during irradiation. Using the Transient Current Technique (TCT) this changing was ascribed to a modification of the electric field in the SDD bulk (Section 4a).
d) Again, the same phenomenon is not observed for neutrons (Section 4b).
e) The initial condition of the electric field (and thus the detector counting rate) can be easily restored by a Bias Voltage inversion (Section 5).

2. Experiment description

The SDD used for the measurement was manufactured by Diamond Detector Ltd. [14]. It has circular gold contacts (SDD-Au) on the both top and bottom surfaces of the diamond plate and features an active area of 4.5×4.5 mm^2 and a thickness of 0.5 mm. The detector is mounted into an aluminium case in order to shield it from electromagnetic interference. Two holes on both sides of the case allow for the alpha particles injection. The radioactive electrodeposited source used for the measurement was ^{241}Am, emitting alpha particles of 5.5 MeV. The source was placed at 9 mm from diamond surface. The measurements were not performed in vacuum, since energy resolution was not the primary goal of this experiment. Therefore, taking into account the alpha energy loss in air the average alpha particle energy is 4.94 MeV. Alpha particles of such an energy have a short interaction range in diamond: about 11.5 μm, which is much less than the detector thickness (500 μm). This means that alpha particles deposit their energy in a thin layer beneath the diamond contact closer to the source. Electrons and holes generated ($E_{e-h} = 13$ eV) in this thin layer are then separated by the applied electric field, E_{bias}, the latter being generated by applying a bias voltage V_{bias} (an ORTEC 710 1 kV Quad bias supply was used). The other contact was connected to the bias supply ground. For instance, $V_{bias} = +400$ V applies an average electric field of 0.8 V/μm. When the source is placed close to the contact at ground, the holes are immediately collected, while electrons travel through the whole detector bulk up to the contact positively biased. The current signal, $i(t)$, induced by the holes and electrons motion inside the detector, is, in this case, almost entirely due to the electron drift. On the other side, when the ^{241}Am source is placed closer to the positively biased contact, the current signal is due to the holes travelling through the whole detector volume.

Two preamplifiers were used: A) a fast shaping preamplifier (20 ns) [15] optimized for spectroscopic measurements (EC1) and B) a current amplifier (DBA IV, 2 GHz BW, gain of 46 dB) [16], used for detailed investigation of the pulse shape (EC2). The signals are digitized, using a 10 bit – 1 GS/s digitizer and a 12 bit – 1.8 GS/s digitizer, respectively, and then processed off-line.

The SDD stability measurements with neutrons were performed at the ISIS-VESUVIO [17] beam line. They were similar to those described in [18] but using EC1. The SDD was placed in neutron beam for about 14 h at a distance of 12.4 m from the ISIS target.

3. Counting stability

3.1. Measurements with alpha particles

Signals from the amplifier are sorted into the Pulse Height (PH) spectrum shown in Fig. 1. The measurement, with the source placed on the positively biased contact, (holes motion), lasted 5 min with $V_{bias} = +400$ V and the count rate was around 90 cps. The spectrum represents the energy deposited into the detector by alpha particles emitted from the ^{241}Am source: the peak is at 4.94 MeV with a Full Width Half Maximum (FWHM) of 150 keV; this gives an energy resolution of 3.0%. Such a value is sufficient for the present purpose.

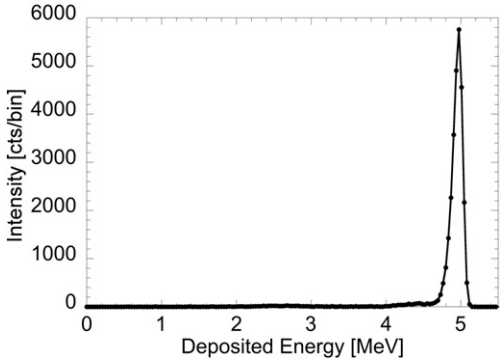

Fig. 1. ^{241}Am Pulse Height (PH) spectrum obtained with the SDD using EC1; the bin width is 35 keV. The measurement lasted 5 min, the energy resolution achieved is 3.0%. The source was placed on the positively biased contact (holes motion).

In order to study the time detector stability during the irradiation time, t_m, a time-resolved analysis of the spectrum in Fig. 1 was performed: as a significant parameter we used the full energy peak intensity. In practise, the peak integral between 4.3 MeV (Lower Threshold Discriminator, LTD) and 5.9 MeV (Upper Threshold Discriminator, UTD) was evaluated over a constant measurement time. At $V_{bias} = +400$ V alpha spectra have been acquired every minute for about 1 h, peak intensity count rate being 90 cps. Results of this analysis are reported in Fig. 2(a), where the normalized count rate is reported as function of the fluence rate. The full black line represents the detector stability obtained at $V_{bias} = +400$ V; the intensity is normalized considering the peak intensity of the first recorded spectrum. At $V_{bias} = +400$ V the SDD peak intensity is constant, meaning that the SDD is stable, up to a fluence of 7×10^3 alphas/mm^2 (about 25 min). After that the intensity of the alpha peak rapidly decreases, as can be seen in Fig. 2(b), where the ^{241}Am spectrum at the beginning of the measurement is compared with the spectrum acquired after a fluence of 10,000 alphas/mm^2, the two spectra are normalized to the same acquisition time. This effect is called polarization effect [20] and it will be discussed later. The irradiation time to get the detector polarized (the counting rate starts to decrease), here called polarization time, is related to the fluence, i.e. to the total charge collected, and V_{bias}, which gives the electric field intensity into the detector bulk, but does not depend on the charge carrier type. In particular the lower is V_{bias} the lower is the polarization time: as an example, if at $+400$ V the polarization time is 20 min, at $+200$ V the polarization time is decreased at 8 min.

3.2. Measurements with fast neutrons

The time-stability of the SDD during the irradiation time with neutrons was studied by counting during 290 s the number of signals whose amplitude was above a threshold of 150 mV (corresponding to a deposited energy equal to 6 MeV). In Fig. 3a the number of counts at different fluence values is reported normalized with respect to the number of counts at the beginning of the measurement. The SDD behaviour is completely different from the one observed during alpha particle irradiation (Fig. 2): the total counts decrease of 20% after a neutron fluence of 1.2×10^6 neutrons/mm^2 (first 50 min). After this transient time the counting rate is constant within 5%. A similar effect was also observed with protons in the MeV energy range [19]. In Fig. 3b the same plot is shown for a Single-crystal Diamond Detector with aluminium contacts

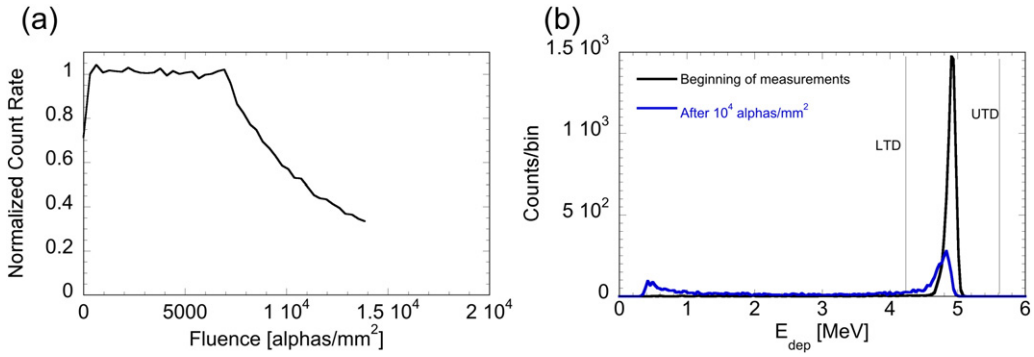

Fig. 2. Stability (a) of the ^{241}Am alpha peak and degradation of the Pulse Height spectrum (b). The integration edges (Lower Threshold Discriminator, LTD, and Upper Threshold Discriminator, UTD) used for the evaluation of the peak integral are also displayed.

(SDD-Al) instead of the gold one. In this case the detector count rate is stable within 5% during the whole measurement.

4. Pulse shape analysis

4.1. Measurements with alpha particles

Using the EC2, the polarization effect can be studied more in detail. Alpha-induced current pulses were acquired and the electric field calculated using the Transient Current Technique (TCT) [21]. This technique is based on the observation of the current signal shape induced by the charge carrier drift inside the detector bulk [22,23],

$$i(t) = Q \cdot v(t)/l \tag{1}$$

where Q is the moving charge, v its velocity and l the distance between the two contacts. Here an approximation (sufficient for the present purpose) was used: $v(t)$ is much smaller than the saturation velocity. In Fig. 4a $i(t)$ induced by electrons drift inside the detector bulk is shown at the beginning of the measurement. The signal starts when the electronic cloud is produced by alpha particle interaction at Time = 0 ns. Values at Time <0 ns represent the baseline. The total signal width represents the electron drift time equal to about 10 ns. The total collected charge Q has been calculated by integrating $i(t)$ and corresponds to $Q = 41.9$ fC. If the electronic cloud is taken as point wise the position of the cloud can be calculated from (1) and can be written as:

$$\frac{x(t)}{l} = \frac{\int_0^t i(t')dt'}{Q} \tag{2}$$

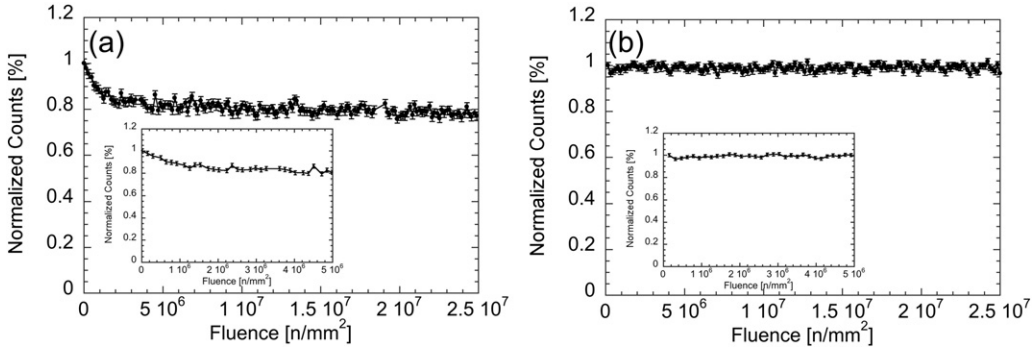

Fig. 3. SDDs stability measured at the ISIS-VESUVIO beam line for the SDD with gold contacts (Au-SDD) (a) and aluminium contacts (Al-SDD) (b).

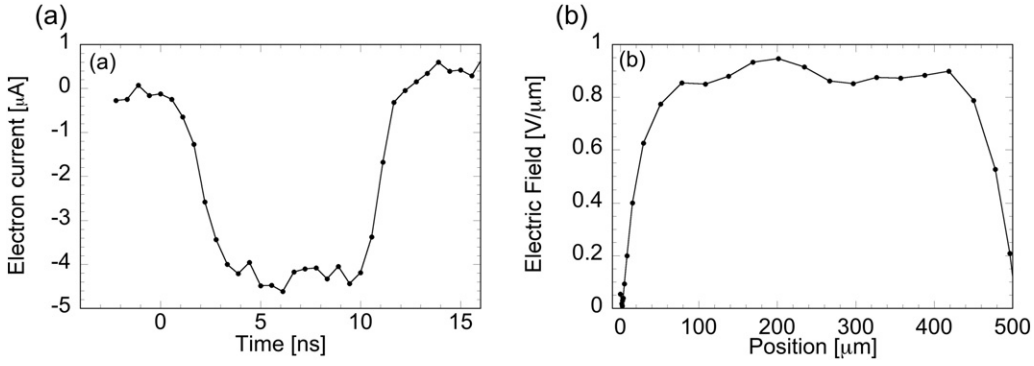

Fig. 4. Electron induced signal measured at the beginning of the measurement is shown in (a); the corresponding electric field calculated using TCT is shown in (b).

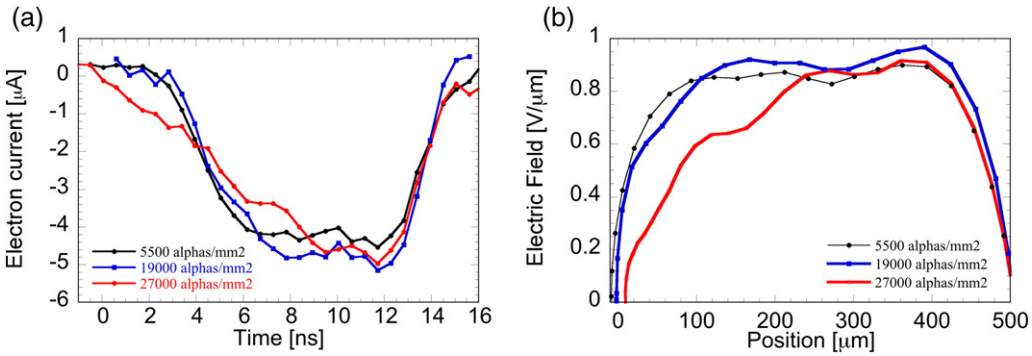

Fig. 5. Same as Fig. 4 but at different fluence values, at 5500, 19,000 and 25,000 alphas/mm^2.

where $x = 0$ μm corresponds to the ground contact, and $x = 500$ μm to the bias contact. The velocity ($v(t)$) can be expressed as function of the position x, and the electric field is given by:

$$E(x) = \frac{v(t(x))}{\mu} \tag{3}$$

where μ is the electron mobility in diamond. The mobility, assumed to be constant, was calculated by integrating the velocity $v(x)$ along the moving direction x divided by V_{bias}. We measured an electron mobility value equal to 630 cm^2/Vs and a mean velocity of 5×10^4 m/s, which are consistent with values obtained in previous studies [24]. The electric field $E(x)$ calculated from signal in Fig. 4a is shown in Fig. 4b. Although the rising and the falling part of the electric field are affected by the limited bandwidth of the electronic chain, we observe that the electric field has "squared" shape. This is ascribed to the space charge absence in the detector bulk: therefore the electric field inside the detector is almost equal to the electric field inside a capacitor.

In Fig. 5 the same as Fig. 4 is reported but at different values of fluence. As it can be easily seen, after 5500 alphas/mm^2 the signal shape and the corresponding electric field are almost equal to those obtained in Fig. 4a–b. With the increase of measurement time, at fluences of 19,000 and 25,000 alphas/mm^2 the shape of signal and electric field is different: from a "squared" shape the electric field changes into a "trapezoidal" shape. The electric field slope (lower at 0 μm and higher at 500 μm) means that a negative space charge is present inside the detector bulk. By increasing the irradiation time the slope is getting higher, i.e. the space charge is increasing. A remark is due, for the calculation of the electric field only signals which refer to a complete collection of the generated carriers, were considered. Signals due to an incomplete charge collection, those that are responsible to the decrease of the peak intensity in Fig. 2a and b, were here neglected.

By inverting the source position (from the ground contact is placed on the positive bias contact) we observe the holes motion inside the detector bulk. The black line in Fig. 6 (a) represents the hole-induced signal just after the source position inversion: due to the higher mobility, hole-induced signals are faster and higher with respect to those induced by electrons. The electric field shown in Fig. 6(b) (Step 1, black line) was calculated using a hole mobility of 950 cm^2/Vs with a mean velocity of 7.6×10^4 m/s, values are consistent to those reported in [24]. By comparing the shape of this electric field with respect to the one reported with the red line in Fig. 5(b) is clear that the electric field shape is independent from the choice of the charge carrier type used for the calculation. By increasing the irradiation time the signal from the "trapezoidal" shape changes into a "squared" shape, blue (Step 2) and red line (Step 3). This means that the holes motion inside the detector bulk compensate the negative space charge previously created by electrons drift.

In Step 4 (green line) after a fluence of 20,000 alphas/mm^2 the electric field is changed again. The holes, after compensating the negative space charge produced by the electrons drift (Step 2 and 3), start to create a positive space charge: the signal (and the electric field) slope is inverted with respect to the one visible in Step 1. Therefore, the polarization is now due to holes trapping and, therefore, the space charge in the detector is positive.

4.2. Measurements with fast neutrons

A measurement on the signal shape induced by neutron interaction in diamond detector bulk has been carried out. The aim of this preliminary study is to compare neutron and alpha-induced signal shape, in order to explain the neutron measurements described in Section 3. The detector coupled to EC2 was placed in the n_TOF (CERN, CH) [25] neutron beam for about one month [26]; in Fig. 7 some signals induced by neutron interaction on ^{12}C are shown.

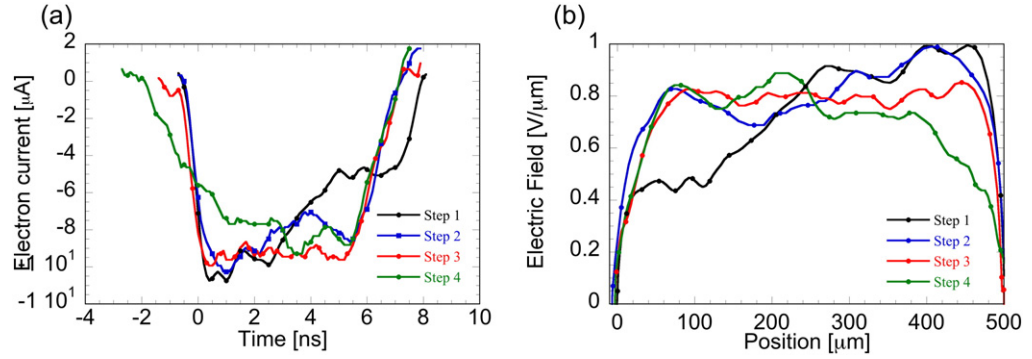

Fig. 6. Same as Fig. 5 but for holes motion obtained after the source position is inverted. Step 1 refers to the measurement taken after the source position inversion. Step 2 corresponds to a fluence of 5900 alphas/mm^2, Step 3 to 13,550 alphas/mm^2, Step 4 to 20,000 alphas/mm^2 after the source position inversion.

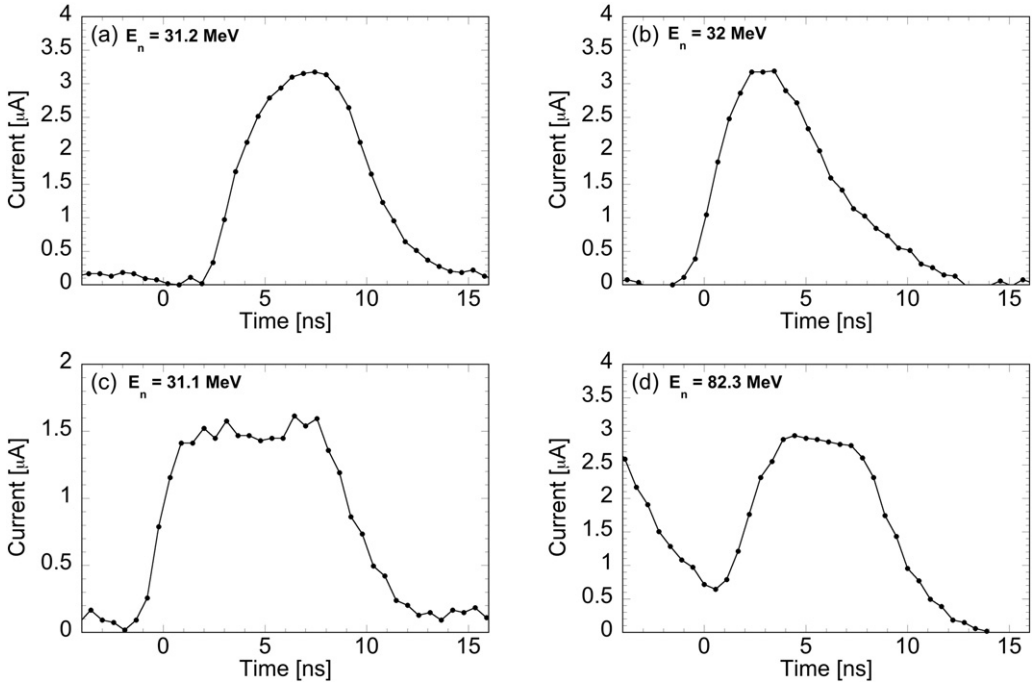

Fig. 7. Neutron induced signals. The corresponding neutron energy is reported in the caption.

In the first three boxes waveforms related to neutron with almost the same collected charge are reported. The shape of the signal here can vary and mostly depends on (i) the position of the neutron interaction with respect to the contact position and (ii) the ionization profile induced by secondary charged particles. The higher is the energy of the secondary products the higher is the range, the less squared the signals is. Pulse shape discrimination has been successfully used as presented in [29]. A rectangular signal, as in (c), means an interaction on the SDD surface due to a charge particle with short ionization range with respect to the detector thickness ("point like interaction"), as was for alphas from ^{241}Am. In the other two cases (a) and (b) the signal has a triangular shape, which corresponds to a long interaction range particle, i.e. the induction signal due to both electrons and holes is now generated during the whole charged particle path, which cannot be considered as point wise with respect to the detector thickness, as in the case of short ionization range. Finally, in (d) a signal of a very high energy neutron (E_n = 82 MeV) is reported. In this case, due to the high range of charged particles produced by neutron interaction, it is likely that the range of charged products is longer than the detector thickness, and therefore only part of the neutron energy is released in the detector.

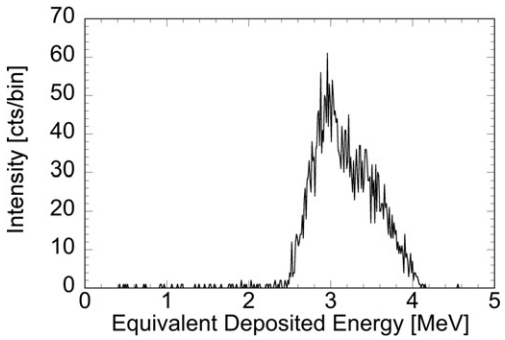

Fig. 8. ^{241}Am alpha spectrum acquired after the polarization effect with no applied voltage.

5. Diamond recovery procedure after polarization

The observation of the diamond polarization effect has been described in the previous sections. In particular, from measurements performed with the fast digital electronic chain and the alpha particles, it was observed that the decrease of the counting rate, shown in Fig. 2, is related to a partial charge trapping, which gives a change in the electric field (Figs. 4–6). Because the external voltage (V_{bias}) is constant during the whole measurements (E_{bias} = 0.8 V/μm), the polarization effect induces an internal radiation-induced electric field E_{pol}. This field partially shields the E_{bias}, and modifies its shape: if the space charge is high enough (alpha fluence >40,000 alphas/mm^2) no signals are collected on the electrode. By placing the alpha source on the other electrode (on the ground contact if polarization was induced by holes as in Section 2) it can be observed that E_{pol} is high enough to collect the e-h produced by the ^{241}Am source even without applying V_{bias}. In Fig. 8 the spectrum has been acquired for 20 s; the counting rate is almost stable within the first 50 s and then exponentially decreases with a time constant of 48 s.

The V_{bias} switching off is not enough to completely restore the detector properties. On the other hand, if a polarity inversion of V_{bias} is performed, the signal and the electric field shape are restored to those in Fig. 4a–b. An example of a cycle of polarity inversion consists of a periodic variation of V_{bias}: 45 min at V_{bias} = +400 V, 30 s at V_{bias} = 0 V, 10 min at V_{bias} = −400 V and then 30 s at V_{bias} = 0 V. Signals have been acquired during the +400 V regime, and the stability of the ^{241}Am peak is evaluated (as in Section 2) during three HV-cycles. In Fig. 9 the source count rate is reported during three cycles of polarity inversion. The source, placed near the positively biased contact, gives a rate of 110 cps and the fluence at which the detector is polarized is reproducible and equal to 7 × 10^3 alphas/mm^2.

6. Discussion

In the previous sections the observation of the polarization effect was described and a simple way to recover the detector properties has been proposed.

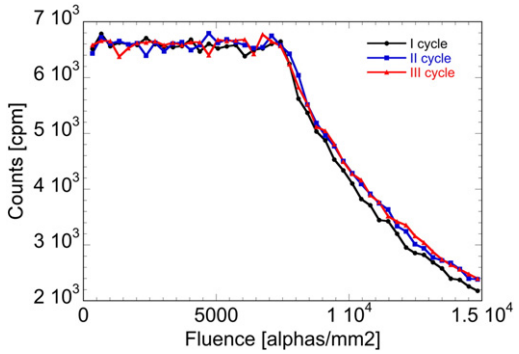

Fig. 9. Stability of the Au-SDD under alpha particle irradiation, the source count rate was 110 cps. The polarization is induced by holes motion and trapping inside the detector. With a polarity inversion of the bias voltage the detector properties are restored.

The fact that with a polarity inversion the polarization effect can be controlled means that this effect is not permanent and is due to charge carriers reversible trapping inside the detector bulk defects. As a matter of fact by inverting the bias polarity the trapped charge can move and is therefore removed. For example, the electrons moving from one contact to the other one can be trapped in the crystal impurities [27], as occurs in polycrystalline diamonds. The presence of this trapped charge inside the detector impurities modifies the space charge profile, which gives rise to a significant deviation from a uniform electric field: the electric field gradually changes from the squared shape to the trapezoidal shape. The electric field generated by trapped charges, E_{pol}, can be high enough to shield the electric field from V_{bias}, In fact, as described in Section 5, without applying V_{bias} is possible to acquire signals, which means that E_{pol} can also prevent the electron drift from one electrode to the other one. The space charge sign is equal to the charge of the moving carrier type. Changing the carrier type, i.e. moving the source, the space charge can be compensated, and the electric field restored.

Neutron measurement revealed a different behaviour: in one case (SDD-Au) the count rate immediately decreases, and then (after about 1 h) is stable for several hours. In the case of SDD-Al the rate is almost constant during the whole measurements. The difference between the behaviour with alpha particles and neutrons is related to ionization range: alpha particles from ^{241}Am (short range) interact near the SDD surface, and there is only one charge carrier type moving inside the detector bulk, the space charge modifies dramatically the electric field. On the other hand, neutrons (long range), can i) interact in the whole volume, therefore, the induction signal is due to both holes and electrons, i.e. the space charge in the detector bulk is due to a combination of positive and negative charge trapped; and ii) the ionization range of the secondary product can be very high compared to the SDD thickness and the signal shape (triangular) cannot be used for electric field calculation as did for ^{241}Am alphas. Once the detector bulk defects are fully filled by charge carriers (both positive and negative) a stable condition is reached, the effective space charge modified the electric field, the count rate has decreased, but the effect on the electric is lower with respect to the case under alpha particle irradiation, and from this point the count rate is almost constant for several hours.

7. Conclusions

SDDs, due to their small size, fast response time and radiation hardness, can play an important role in fusion and spallation neutron sources experiments. Recent experiments confirm the SDD capability to perform neutron spectroscopy with a good energy resolution at high rates.

In this paper a pulse shape analysis in SDD has been carried out. The signal shape has been studied using both ^{241}Am alpha particles and spallation neutrons. Measurements performed with alpha particles underlined the SDD polarization effect feature. We interpret this to be due to a partial and reversible charge trapping. Trapping modifies the fixed charge distribution into the detector bulk resulting in a change of the electric field. The detector properties can be restored with a polarity inversion of the bias voltage.

References

[1] C.D. Frost, S. Ansell, G. Gorini, A new dedicated neutron facility for accelerated SEE testing at the ISIS facility, Reliability Physics Symposium, 2009 IEEE International, IEEE, 2009.
[2] E. Normand, Single event upset at ground level, IEEE Trans. Nucl. Sci. 43 (1996) 2742.
[3] P.E. Dodd, M.R. Shaneyfelt, J.R. Schwank, G.L. Hash, Neutron-induced soft errors, latchup, and comparison of SER test methods for SRAM Technologies, Proceedings of the International Electron Device Meeting 2002, pp. 333–336.
[4] A. Pietropaolo, et al., Single-crystal diamond detector for time-resolved measurements of a pulsed fast-neutron beam, Europhys. Lett. 92 (2010) 68003.
[5] A. Pietropaolo, et al., Fission diamond detectors for fast-neutron ToF spectroscopy, Europhys. Lett. 94 (2011) 62001.
[6] M. Rebai, et al., Fission diamond detector tests at the ISIS spallation neutron source, nuclear physics B proceedings 2011, pp. 313–315.
[7] C. Cazzaniga, et al., Single crystal diamond detector measurements of deuterium-deuterium and deuterium-tritium neutrons in Joint European Torus fusion plasmas, Rev. Sci. Instrum. 85 (4) (2014) 043506.
[8] M. Nocente, et al., Fast ion energy distribution from third harmonic radiofrequency heating measured with a single crystal diamond detector at JET, J. Sci. Instrum. 86 (2015) 103501.
[9] M. Pillon, et al., 14 MeV neutron spectra measurements with 4% energy resolution using a type IIa diamond detector, Nucl. Instrum. Methods Phys. Res., Sect. B 101 (4) (1995) 473–483.
[10] C. Cazzaniga, et al., A diamond based neutron spectrometer for diagnostics of deuterium-tritium fusion plasmas, Rev. Sci. Instrum. 85 (11) (2014) 11E101.
[11] M. Girolami, et al., Mosaic diamond detectors for fast neutrons and large ionizing radiation fields, Phys. Status Solidi (2015) (a).
[12] M. Rebai, et al., Pixelated single-crystal diamond detector for fast neutron measurements, J. Instrum. 10 (03) (2015), C03016.
[13] M. Osipenko, et al., Single-crystal diamonds for neutrons, Eur. Phys. J. E Plus 129 (12) (2014) 1–8.
[14] Diamond Detector Ltd. BCMS-SCD464650A - BCM.
[15] CIVIDEC instrumentation webpage, http://www.cividec.at/#home.html
[16] P. Moritz, Broadband Preamplifiers for Fast Particle Detectors, GSI - Gesellschaft für Schwerionenforschung mbH, Planckstr. 1, D-64291 Darmstadt, Germany.
[17] ISIS-VESUVIO beamline at the Rutherford Appleton Laboratory webpage, http://www.isis.stfc.ac.uk/instruments/Vesuvio/.
[18] M. Rebai, et al., Diamond detectors for fast neutron measurements at pulsed spallation sources, J. Instrum. 7 (2012) C05015.
[19] Y. Sato, et al., Radiation hardness of a single crystal CVD diamond detector for MeV energy protons, Nucl. Instrum. Methods Phys. Res., Sect. A 784 (2015) 147–150.
[20] M. Guthoff, et al., Radiation damage in the diamond based beam condition monitors of the CMS experiment at the Large Hadron Collider (LHC) at CERN, Nucl. Instrum. Methods Phys. Res., Sect. A A730 (2013) 168–173.
[21] M. Lampert, P. Mark, Current Injection in Solids, Academic, New York, 1970.
[22] S. Ramo, Currents induced by electron motion, Proc. Of the I.R.E., 1939.
[23] W. Shockley, Currents to conductors induced by a moving point charge, J. Appl. Phys. 9 (1938) 635.
[24] H. Pernegger, et al., Charge-carrier properties in synthetic single-crystal diamond measured with the transient-current technique, J. Appl. Phys. 97 (2005) 073704.
[25] C. Guerrero, et al., Performance of the neutron time-of-flight facility n_TOF at CERN, Eur. Phys. J. A 49 (2) (2013) 1–15.
[26] M. Rebai, et al., Response of a single-crystal diamond detector to fast neutrons, J. Instrum. 8 (2013) P10007.
[27] C. Manfredotti, et al., IBIC investigation of radiation-induced effects in CVD and natural diamond, Nucl. Instrum. Methods Phys. Res., Sect. A 426 (1999) 156.
[29] P. Kavrigin, P. Finocchiaro, E. Griesmayer, E. Jericha, A. Pappalardo, C. Weiss, Pulse-shape analysis for gamma background rejection in thermal neutron radiation using CVD diamond detectors, Nucl. Instrum. Methods Phys. Res., Sect. A (2015).